Retinoic acid controls vascular formation by activating transcription of aryl hydrocarbon receptor gene in medakafish *Oryzias latipes*

Naotaka Sada, Takahiro Hanafusa, Yuichi Onizuka, Yasufumi Hayashida, Shota Kageyama, and Ichiro Yamashita*

Center for Gene Science, Hiroshima University, Kagamiyama 1-4-2, Higashihiroshima 739-8527, Japan.

* Correspondence: iyama@hiroshima-u.ac.jp

SUMMARY

Retinoic acid (RA) has been shown to have a role in vascular formation, but how it affects is not fully understood. Previously, we reported that RA and its nuclear receptor (RAR) is required for transcription of *ahr1* encoding an aryl hydrocarbon receptor (AHR), and that pharmacological modulation of RA, RAR, and AHR impairs the formation of common cardinal veins (CCVs) on the yolk of medakafish embryos. Here, to delineate a role for *ahr1* in the vascular formation, we used an antisense-*ahr1* mRNA to suppress *ahr1*. Following the development of *vegfr1*-expressing angioblast cells, we show that the antisense-*ahr1* greatly inhibited the accumulation of angioblasts at the prospective branchial arch (PBA) where CCVs begin to develop on the yolk and the following CCV formation, demonstrating for the first time the essential role of *ahr1* in the embryonic vascular formation of vertebrates. We also show that *rarα* and *ahr1* mRNAs are co-expressed at PBA, suggesting a possible role of the specific expression.

KEY WORD: aryl hydrocarbon receptor, common cardinal vein, retinoic acid, retinoic acid receptor, medakafish

INTRODUCTION

Vitamin A (retinol) is essential for embryonic development and tissue differentiation in adult organisms (Clagett-Dame & Knutson, 2011; Rhinn & Dollé, 2012). It is not synthesized *de novo* by vertebrates and is acquired from the diet. Retinoids are deposited in eggs during oogenesis (Levi *et al*., 2012). Retinal, a metabolite of retinol by alcohol/retinol dehydrogenases, is the predominant

retinoid storage in eggs and oocytes of lower vertebrates (fish, amphibians, and reptiles), in contrast to higher vertebrates (birds and mammals), where retinol is the major retinoid used by embryos. Retinal is further metabolized during early embryonic development by retinal aldehyde dehydrogenase (RALDH) to retinoic acid (RA), which enters the nucleus and activates nuclear retinoid receptors (RARs). They regulate transcription of many key target genes for cardiovascular, ocular, and central nervous systems, limb, and trunk (Duester, 2008). Previously, we reported in medakafish (Hayashida et al., 2004) that RA and RAR are required for embryonic development of common cardinal veins (CCVs) which collect all the blood from the embryo and transport it back to the heart (Fujita et al., 2006) and for transcription of aryl hydrocarbon receptor (AHR) gene (*ahr1*) (Kawamura & Yamashita, 2002).

AHR is also conserved among vertebrates and is expressed during embryonic development and in a variety of adult tissues (Barouki, et al., 2007). Although it is a well-known ligand-activated transcription factor mediating not only most of the toxic and carcinogenic effects of a wide variety of environmental contaminants such as dioxin but also xenobiotic-detoxifying function by activating transcription of a battery of cytochrome P450 genes such as *cyp1a* (Hankinson, 1995; Carney et al., 2006), those could be late-acquired property that might have been added to original physiological functions. Phenotypic alterations found in mice lacking *ahr* expression have provided strong support for the involvement of the AHR in cell physiology such as hepatic, hematopoietic, cardiovascular and immune systems (Fernandez-Salguero et al., 1995). Recent investigations are discovering new insights dealing with cell differentiation and pluripotency, chromatin dynamics, activation of mobile genetic elements, proliferation, epidermal barrier function and immune regulation (Mulero-Navarro & Fernandez-Salguero, 2016). Moreover, the genetic characterization of AHR in invertebrates such as the fly *Drosophila melanogaster* (Céspedes et al., 2010) and the worm *Caenorhabditis elegans* (Qin & Powell-Coffman, 2004; Qin et al., 2006) has provided evidence for its developmental roles.

Previously, we proposed a feedback mechanism regulating *in vivo* RA levels, in which excessive synthesis of RA activates *ahr1* mRNA expression, then, increased activity of AHR in turn stimulates conversion of RA to inactive metabolites (Hayashida et al., 2004). We also reported the physiological significance of the RAR-mediated expression of *ahr1* in the CCV formation of medaka embryos by exploring pharmacological studies with antagonists specific

to RAR and AHR. Our model suggests two routes through which hyperactivation of AHR by binding to dioxin abrogates vascular formation: one giving rise to RA-deficiency that is generally accepted in mammals (Andreola *et al*., 1997) and another excessively activating the proper way to vascular formation. However, this model is not genetically verified.

Here we show that antisense-*ahr1* greatly inhibited the formation of CCVs, demonstrating for the first time the essential role of *ahr1* in the embryonic vascular formation of vertebrates. *In situ* hybridization experiments revealed that *rarα* and *ahr1* mRNAs are co-expressed at the prospective branchial arch (PBA) where CCVs begin to develop on the yolk. Furthermore, RA-sensitive period for the expression of both mRNAs was the same as that for CCV formation in the time-lapse experiments, suggesting the possible role of the co-expression at PBA in the CCV formation.

MATERIALS AND METHODS

Fish, embryo, and exposure to reagent.

We used the d-rR strain of medaka fish, *O. latipes* (Kawahara and Yamashita, 2000). The fish were maintained at 25 – 26^{o}C under artificial photo-period of 14L:10D, and fed by powdered Tetramin (Tetra). Fertilized eggs were collected before 10 hpf, rinsed and immersed in Yamamoto's salt solution (Yamamoto, 1969) containing NaCl (7.5 g/l), KCl (0.2 g/l), $CaCl_2.2H_2O$ (0.265 g/l), and $NaHCO_3$ (0.02 g/l), and exposed to test reagents from 10 hpf. All reagents were purchased from Sigma except for the antagonist of RAR, Ro41-5253, kindly provided by E.-M. Gutknecht (F. Hoffmann-La Roche Ltd, Basel). Reagents were dissolved in dimethyl sulfoxide or ethanol, and stored at –80^{o}C. Stock solutions were diluted over 1,000-fold with Yamamoto's solution before use. The solvents were added to the mock-treated eggs as controls. Eggs were incubated at 25 – 26^{o}C under shading with alminum foil and inspected for vascular development under a dissecting microscope at 3 dpf as described (Hayashida *et al*., 2004). Experiments were done at least 3 times in which unit samples contained more than 30 or approximately 50 eggs for observation of vascular development or extraction of total RNA, respectively. Percent embryos with vascular damages were presented as mean±SEM. Statistical significance between values of control and experiment was assessed by Student's *t*-test.

RT-PCR.

Total RNA was extracted using NucleoSpin kit (Macherey-Nagel) after homogenization of embryos with pellet mixers. RT-PCR analysis was done using Ready-To-Go RT-PCR beads (GE Healthcare) or by two-step reactions, first with reverse transcriptase (ReverTra Ace, Toyobo) using oligo-dT as a primer and then with DNA polymerase (Ex Taq, Takara). PCR was done at least 5 times for each RNA sample at optimal and suboptimal cycle numbers with gene-specific primers as follows: ***ahr1*****,** forward primer (F) 5'-CCAGCAGGAGTTCAGGAGGA-3', reverse primer (R) 5'-ATTTTACCCTTTGCGTCACA-3'. Annealing at 60^{o}C for 30 sec, extension at 72^{o}C for 1 min, 431-bp amplified DNA. ***raldh2*****,** F 5'-ATCCCCGGAGCGGTGAAG-3', R 5'-TCCTTGGAGGTCAACAAACA-3'. Annealing at 55^{o}C for 30 sec, extension at 72^{o}C for 1 min, 405-bp amplified DNA. ***rarα*****,** F 5'-AAGCAGGAGTGCACG-3', R 5'-GGTCAATGTCCAAGGAA-3'. Annealing at 60^{o}C for 30 sec, extension at 72^{o}C for 1 min, 160-bp amplified DNA. **β-actin,** F 5'-GGTATCGTCATGGACTCT-3', R 5'-GGTGATGACCTGTCCGTCAG-3'. Annealing at 55^{o}C for 30 sec, extension at 72^{o}C for 1 min, 300-bp amplified DNA. ***cyp1a*****,** F 5'-GCACAGACCAAGCAG-3', R 5'-ACTGGAAGCGGTTGT-3'. Annealing at 50^{o}C for 30 sec, extension at 72^{o}C for 1 min.

After electrophoresis in agarose gel, amplified DNAs were stained with ethidium bromide and photographed. DNA bands were scanned with GT-9700F scanner (Epson), adjusted using software (Adobe Photoshop Elements 3.0), and analyzed for intensity with Scion Image software. Statistical significance was assessed by Student's *t*-test.

Whole-mount *in situ* hybridization.

Whole-mount *in situ* hybridization was performed essentially as described (Inohaya, 1997). Embryos were treated with cycloheximide (50 or 100 mg/l) to stabilize *ahr1* and *raldh2* mRNAs for 5 h before fixation. The cDNAs used as a template for preparation of probes were cloned in the following plasmids: *ahr1* (pOL97 or pOL100 for antisense, pOL102 for sense); *hoxa3a* (pOL145); *krox20* (pOL150); *raldh2* (pOL155); *rarα* (pOL151); *rarγ1* (pOL167); and *vegfr1* (pOL121 for sense, pOL122 for antisense).

Electroporation.

The procedure was schematically presented in Fig. S1. Less than 20 embryos (1- to 4-cell stage) were immersed in a drop (40 µl) on Petri dish of the 10-fold concentration of Yamamoto's solution containing each or combination of the plasmid DNAs (pOL21, pYO4, and pYO5) in the concentration of 0.5 µg/µl each. The plasmid pOL21 (Kawamura *et al*., 2002) was used for expression of green fluorescent protein (GFP-S65T). The plasmid pYO4 was used for expression of AHR1. The plasmid pYO5 was used for expression of antisense-*ahr1* RNA from the entire sequence of the *ahr1* cDNA (Kawamura & Yamashita, 2002). Every expression is driven by the medaka β-actin promoter (Hamada *et al*., 1998). The egg envelope was perforated with a sewing needle, resulting in the penetration of the plasmid DNA into the fluid between the egg envelope and the embryo by osmotic pressure. Then, 20 ml of Yamamoto's solution was poured onto the Petri dish, a portion (approximately 400 µl) of which, together with the eggs, was transferred into a cuvette for electroporation. Electroporation was carried out using ElectroSquarePorator T820 (BTX) under the following condition: voltage, 12 - 15 V; burst duration, 10 ms; burst interval, 1.0 sec; number of burst, 3. After putting back to the Petri dish, eggs were incubated with or without addition of reagents (β-naphthoflavone and DEAB) at 10 hpf. GFP-expressing embryos (approximately 20% of the treated embryos) were collected at 35 hpf for extraction of total RNA, at 2 dpf for *in situ* hybridization of *vegfr1*$^{+}$ angioblasts, and at 3 dpf for observation of vascular damages. Statistical significance was assessed by Chi-square test.

RESULTS

Development of CCV revealed by *vegfr1* expression

To explore the development of CCVs, we visualized angioblasts by *in situ* hybridization using as a probe the medaka cDNA (*vegfr1*) (Hayashida *et al*., 2004) encoding vascular endothelial growth factor receptor (VEGFR) (Fig. 1A). We observed that angioblasts first appeared at 28 hpf, arranged at periphery of embryonic body in two parallel stripes. By 36 hpf, the anterior haemangioblasts accumulated at the prospective branchial arch (PBA) at the level of rhombomere 7 (r7) (closed arrowhead), where CCVs begin to develop on the yolk. CCVs began to form on most embryos by 40 hpf (Fig. 1B) and reached to head by 48 hpf before start of circulation at 53-55 hpf. Primordial hindbrain channels (open

arrowhead) formed by 36 hpf. Intersomite vessels also appeared at 46 hpf (bracket).

RA controls CCV formation

To explore whether RA controls the development of *vegfr1*-expressing (*vegfr1*+) angioblast cells, we first treated the 10-hpf embryos with diethyl aminobenzaldehyde (DEAB), a specific inhibitor of RALDH (Hayashida *et al*., 2004) (Fig. 2A). There was no effect on the development of angioblasts at 30 hpf. However, the drug specifically inhibited the accumulation of angioblasts at PBA at 36 hpf and the formation of CCV by 48 hpf, while there was no effect on the vessel formation in the brain and somites (open arrowhead). The treatment also caused anterior shift of somites up to the position marked by arrows, indicating that embryos developed in the RA-deficient condition (Dubrulle & Pourquié, 2004). These results indicate that RA is specifically required for the formation of angioblast clusters at PBA and the following CCV formation. We also examined the effect of excess RA by treating the 10-hpf embryos with 10 nM RA (Fig. 2A). It reduced the level of *vegfr1* signals at the anterior brain where morphogenesis was appreciably affected (open arrowhead), and also inhibited the formation of CCV, while excess angioblasts were present at PBA (closed arrowhead). These results indicate that precise control of RA concentration is critical for the CCV formation.

To analyze when RA is required for CCV formation, staged embryos were treated with DEAB and examined at 48 hpf for *vegfr1*-expressing CCV. Half of the embryos became insensitive to DEAB around 24 hpf (Fig. 2B), indicating that RA is required for CCV formation during the mid- to late-gastrula stage (Iwamatsu, 2004).

RA controls *ahr1* mRNA expression directly

We first examined transcript levels of *ahr1*, RA-related genes *raldh2* (retinal aldehyde dehydrogenase) and *rarα* (RA receptor α), and β-actin gene as a control by RT-PCR of RNAs extracted from blastula- to somite-stage embryos (Fig. 3A). The *ahr1* mRNA was detected during all the stages examined and its level increased after 19 hpf. The *raldh2* and *rarα* mRNAs were rarely detected by 16 hpf but increased sharply after 19 hpf. These results are consistent with the previous observation that RA and its receptor RAR control transcription of *ahr1* (Hayashida *et al*., 2004) and suggest that *in vivo* levels of RA increase at the

mid-gastrula stage in medakafish embryos as in other vertebrates (Duester, 2008; Lloret-Vilaspasa *et al*., 2010).

We next investigated whether RA activates transcription of *ahr1* directly. To test this, the 22-hpf embryos were first treated with cycloheximide (CHX) for 1 h, then added with RA. After 5-h incubation, RNA was extracted and analyzed for *ahr1* mRNA by RT-PCR. Addition of RA enhanced transcript levels of *ahr1* in the presence and absence of the protein synthesis inhibitor (Fig. 3B), indicating that RA activates transcription of *ahr1* directly.

RA controls *ahr1* mRNA expression at PBA

We analyzed *ahr1* mRNA expression by *in situ* hybridization (Fig. 4A). Signals for *ahr1* mRNA first appeared at 42 hpf on the surface of anterior brain and eye and at PBA which ranges from r7 to r8 (bracket). The expression at PBA became increasing by 48 hpf. Expressions in otic vesicles, rhombomere, and somite are not constant. There was no specific signal using a sense probe.

To investigate whether the *ahr1* mRNA expression at PBA is related to CCV formation, we examined correlation between the *ahr1* expression levels and the *in vivo* RA levels that affect CCV formation (Fig. 4B). By treatment with a lower concentration of DEAB (2 μM) that inflicts only minor vascular damages (Hayashida et al., 2004), *ahr1* signal at PBA was decreased but significant amounts of the signal remained at the periphery of posterior hindbrain (bracket). However, no signal was detectable by treatments with higher concentrations of DEAB (5 and 10 μM) that abolish CCV formation.

We next examined the developmental period during which RA is required for *ahr1* expression at PBA (Figs. 4C, D). Staged embryos were treated with 10 μM DEAB and analyzed at 48 hpf for *ahr1* expression at PBA. The 10- to 20-hpf embryos did not express *ahr1* signal at PBA but the later ones expressed significant amounts of *ahr1* signal at PBA (bracket). These results indicate that RA is required for *ahr1* expression at PBA before 25 hpf (late gastrula stage), the same period as for *vegfr1*-expressing CCV formation (Fig. 2B).

Together, these results suggest that RA controls CCV formation through *ahr1* expression at PBA.

RA may control *ahr1* expression through RARα at PBA

We first analyzed by *in situ* hybridization mRNA expression of *krox20*, *raldh2*, and *hoxa3a* as controls. *krox20* was expressed at r3 and r5 in the hindbrain

(Schilling & Kinght, 2001), and *raldh2* in the somite (Dobbs-McAuliffe, 2004) (Fig. 5A). *hoxa3a* was expressed at r5 and from r7 to r8 (r7-r8) (Fig. 5B). It's expression at r7-r8 was activated by RA and decreased by DEAB (Fig. 5B), indicating positive control of *hoxa3a* by RA as expected (Schilling & Kinght, 2001). Expression of *raldh2* was increased by the treatments with DEAB and an RARα antagonist (Ro41-5253) (Fig. 5C), indicating negative control of *raldh2* by RA (Dobbs-McAuliffe *et al*., 2004). As expected, we also noted body axis malformation such as anterior and posterior shift of hindbrain by the treatments with RA and DEAB, respectively (Schilling & Kinght, 2001), and anterior shift of somite by DEAB and the antagonist (Duester, 2007).

Next, we examined expressions of *rarα* and *rarγ1* to explore what kinds of RAR activate transcription of *ahr1*. *rarα* was expressed at r7-r8 and co-expressed weakly with *ahr1* at the periphery of the hindbrain (Fig. 5A). *rarγ1* was expressed at PBA at the level of r5 (Fig. 5D). To investigate whether RA controls expression of *rarα* and *rarγ1*, 10-hpf embryos were treated with DEAB and examined at 36 hpf. The drug completely abolished *rarα* expression at the posterior hindbrain and its periphery, however, did not affect expression of *rarγ1* (Fig. 5D). Increasing concentrations of DEAB caused posterior shift of *krox20* and reduced expression of *rarα* more severely, which were recovered by addition of RA (Fig. 5E). In reciprocal experiments by adding excess RA, we observed anterior shift of *krox20* and enhanced expression of *rarα* (Fig. 5F). These results indicate that RA activates *rarα* expression.

We next examined the RA-sensitive period for *rarα* expression. Staged embryos were treated with 10 μM DEAB and analyzed at 36 hpf. The 10- to 18-hpf embryos did not express *rarα* but those from 26 hpf on expressed it, indicating that RA is required for *rarα* expression before 26 hpf (late gastrula stage) (Fig. 5G), the same period as for *ahr1* expression at PBA (Fig. 4C) and for *vegfr1*-expressing CCV formation (Fig. 2B).

Collectively, these results suggest that RA may directly control *ahr1* expression at PBA through RARα.

ahr1 is required for CCV formation

We set up genetic systems for investigating functional roles of *ahr1*. We first identified *cyp1a* as a target of AHR by the observation that increasing concentrations of β-naphthoflavone (β-NF), an agonist of AHR (Hayashida *et al*., 2004), activated *cyp1a* expression more strongly (Fig. 6A). Next, we constructed

three plasmids pYO4, pYO5, and pOL21, expressing under the control of β-actin promoter full-length *ahr1* mRNA, antisense *ahr1* RNA, and as a control green fluorescent protein (GFP-S65T). Finally, we developed an efficient method for introducing DNA into medakafish embryos by electroporation (Fig. S1). Introduction of pYO4 enhanced *cyp1a* expression (Fig. 6B), revealing the authentic activity of the *ahr1*. We also observed that introduction of pYO5 reduced the expression level of *cyp1a* (Fig. 6C), demonstrating the inhibitory activity of the antisense DNA.

To investigate whether *ahr1* is required for vascular formation, we introduced sense and antisense *ahr1* into embryos, and examined vascular damages such as malformation of CCV and blood clotting. We observed only minor effects of antisense *ahr1* but no effect of sense *ahr1* (Fig. 6D). We also investigated the synergistic action of antisense *ahr1* with DEAB since previous studies indicated that co-treatments of AHR antagonist with DEAB enhanced vascular damages (Hayashida *et al*., 2004). We observed that the antisense *ahr1* clearly damaged vascular formation in the presence of DEAB (2 μM) that alone did not show any effect (Fig. 6D).

We also observed that antisense *ahr1* caused a loss of *vegfr1*-expressing CCV in the presence of DEAB (2 μM), which was recovered by co-introduction of sense *ahr1* (Figs. 6E, F). These results confirm that *ahr1* is required for CCV formation. We further investigated whether RA acts only through *ahr1* expression in the CCV formation. If it would do so, expression of *ahr1* by β-actin promoter would cancel the defect caused by higher concentration of DEAB (10 μM). However, the forced expression of *ahr1* did not rescue the defect in CCV formation (Fig. 6G), suggesting the possibility that RA acts not only through *ahr1* but in multiple pathways or that proper activation of *ahr1* at PBA is necessary for CCV formation.

DISCUSSION

We have analyzed the CCV formation of *vegfr1*-expressing angioblast cells. We noticed that the angioblast cells accumulated at PBA before development of CCV formation. RA was specifically required for the accumulation of angioblasts at PBA, where *rarα* and *ahr1* mRNAs were co-expressed in RA-dependent manner. We also verified by using antisense *ahr1* that *ahr1* is required for the accumulation of angioblasts at PBA and subsequent CCV formation. We propose a model for RA action in CCV formation that RA activates transcription

of *rarα* which directly activates *ahr1* expression at PBA (Fig. 7). Currently we do not know how AHR acts at PBA for CCV formation. However, recent reports suggest an interesting speculation. Mathew *et al*. (2008) reported that toxic effect of TCDD in zebrafish fin regeneration is mediated through hyperactivation of Wnt signaling, proposing a novel crosstalk between AHR and Wnt signaling. Kazanskaya et al. (2008) reported that Wnt signaling promotes angioblast and vascular development in vertebrates by activating expression of VEGF. This growth factor binds to and activates VEGFR in angioblasts, and stimulates their proliferation, migration, and survival during vasculogenesis (the formation of blood vessels from *de novo* generation of endothelial cells) and angiogenesis (the process of new blood vessel formation from the pre-existing vessels) (Apte, 2019). Accordingly, we assume that AHR at PBA stimulates production of VEGF which accumulates angioblasts by activating proliferation of angioblasts or their migration to PBA (Fig. 7). The accumulation of angioblasts at PBA, which occurs also in zebrafish embryos before starting CCV formation (Helker *et al*., 2013), may be the first step for the following development of CCV formation. However, it was reported recently that triple AHR mutant zebrafish (*ahr1a*, *ahr1b*, and *ahr2*) are viable with no obvious abnormalities in vascular patterning during embryonic development (Sugden *et al*., 2017).

ACKNOWLEDGEMENTS

We thank E.-M. Gutknecht (F. Hoffmann-La Roche Ltd, Basel) for kindly providing Ro41-5253, K. Kitamura, and N. Tanaka for discussions. This work was supported in part by a grant from the Ministry of Education, Science, Sports and Culture of Japan.

REFERENCES

Andreola, F., F.-Salguero, P. M., Chiantore, M. V., Petkovich, M., Gonzalez, F. J., & De Luca, L. M. Aryl hydrocarbon receptor knockout mice (AHR-/-) exhibit liver retinoid accumulation and reduced retinoic acid metabolism. Cancer Res. 57: 2835-2838 (1997).

Apte, R. S., Chen, D. S., & Ferrara, N. VEGF in signaling and disease: beyond discovery and development. Cell 176: 1248-1264 (2019).

Barouki, R., Coumoul, X., & Fernandez-Salguero, P. M. The aryl hydrocarbon receptor, more than a xenobiotic-interacting protein. FEBS Letters 581: 3608-3615 (2007).

Carney, S. A., Prasch, A. L., Heideman, W., & Peterson, R. E. Understanding dioxin developmental toxicity using the zebrafish model. Birth Defects Res. (Part A) 76: 7-18 (2006).

Céspedes, M. A., Galindo, M. I., & Couso, J. P. Dioxin toxicity *in vivo* results from an increase in the dioxin-independent transcriptional activity of the aryl hydrocarbon receptor. PLoS ONE 5: e15382 (2010).

Clagett-Dame, M., & Knutson, D. Vitamin A in reproduction and development. Nutrients 3: 385-428 (2011).

Dobbs-McAuliffe, B., Zhao, Q., & Linney, E. Feedback mechanisms regulate retinoic acid production and degradation in the zebrafish embryo. Mech. Dev. 121: 339-350 (2004).

Dubrulle, J., & Pourquié, O. Coupling segmentation to axis formation. Development 131: 5783-5793 (2004).

Duester, G. Retinoic acid regulation of the somitogenesis clock. Birth Defects Res. (Part C) 81: 84–92 (2007).

Duester, G. Retinoic acid synthesis and signaling during early organogenesis. Cell 134: 921-931 (2008).

Fernandez-Salguero, P., Pineau, T., Hilbert, D. M., McPhail, T., Lee, S. S., Kimura, S., Nebert, D. W., Rudikoff, S., Ward, J. M., Gonzalez, F. J. Immune system impairment and hepatic fibrosis in mice lacking the dioxin-binding Ah receptor. Science 268: 722-726 (1995).

Fujita, M., Isogai, S., & Kudo, A. Vascular anatomy of the developing medaka, *Oryzias latipes*: a complementary fish model for cardiovascular research on vertebrates. Dev. Dynamics 235: 734-746 (2006).

Hamada, K., Tamaki, K., Sasado, T., Watai, Y., Kani, S., Wakamatsu, Y., Ozato, K., Kinoshita, M., Kohno, R., Takagi, S., & Kimura, M. Usefulness of the medaka β-actin promoter investigated using a mutant GFP reporter gene in transgenic medaka (*Oryzias latipes*). Mol. Mar. Biol. Biotech. 7: 173-180 (1998).

Hankinson, O. The aryl hydrocarbon receptor complex. Annu. Rev. Pharmacol. Toxicol. 35: 307-340 (1995).

Hayashida, Y., Kawamura, T., Hori-e, R., & Yamashita, I. Retinoic acid and its receptors are required for expression of aryl hydrocarbon receptor mRNA and embryonic development of blood vessel and bone in the medaka fish, *Oryzias latipes*. Zool. Sci. 21: 541-551 (2004).

Helker, C. S. M., Schuermann, A., Karpanen, T., Zeuschner, D., Belting, H. -G., Affolter, M., Schulte-Merker, S., & Herzog, W. The zebrafish common cardinal veins develop by a novel mechanism: lumen ensheathment. Development 140: 2776-2786 (2013).

Inohaya, K., Yasumasu, S., Araki, K., Naruse, K., Yamazaki, K., Yasumasu, I., Iuchi, I, & Yamagami, K. Species-dependent migration of fish hatching gland cells that commonly express astacin-like proteases in common. Dev. Growth Differ. 39: 191-197 (1997).

Iwamatsu, T. Stages of normal development in the medaka *Oryzias latipes*. Mech. Dev. 121: 605-618 (2004).

Kawahara, T., & Yamashita, I. Estrogen-independent ovary formation in the medaka fish, *Oryzias latipes*. Zool. Sci. 17: 65-68 (2000).

Kawamura, T. & Yamashita, I. Aryl hydrocarbon receptor is required for prevention of blood clotting and for the development of vasculature and bone in the embryos of medaka fish, *Oryzias latipes*. Zool. Sci. 19: 309-319 (2002).

Kazanskaya, O., Ohkawara, B., Heroult, M., Wu, W., Maltry, N., Augustin, H. G., & Niehrs, C. The Wnt signaling regulator R-spondin 3 promotes angioblast and vascular development. Development 135: 3655-3664 (2008).

Levi, L., Ziv, T., Admon, A., Levavi-Sivan, B., & Lubzens, E. Insight into molecular pathways of retinal metabolism, associated with vitellogenesis in zebrafish. Am. J. Physiol. Endocrinol. Metab. 302: E626-E644 (2012).

Lloret-Vilaspasa, F., Jansen, H. J., De Roos, K., Chandraratna, R. A. S., Zile, M. H., Stern, C. D., & Durston, A. J. Retinoid signaling is required for information transfer from mesoderm to neuroectoderm during gastrulation. Int. J. Dev. Biol. 54: 599-608 (2010).

Mathew, L. K., Sengupta, S. S., LaDu, J., Andreasen, E. A., & Tanguay, R. L. Crosstalk between AHR and Wnt signaling through R-Spondin1 impairs tissue regeneration in zebrafish. FASEB J. 22: 3087-3096 (2008).

Mulero-Navarro, S., & Fernandez-Salguero, P. M. New trends in aryl hydrocarbon receptor biology. Front. Cell Dev. Biol. 4: Article 45 (2016).

Qin, H., & Powell-Coffman, J. A. The *Caenorhabditis elegans* aryl hydrocarbon receptor, AHR-1, regulates neuronal development. Dev. Biol. 270: 64-75 (2004).

Qin, H., Zhai, Z., & Powell-Coffman, J. A. The *Caenorhabditis elegans* AHR-1 transcription complex controls expression of soluble guanylate cyclase genes in the URX neurons and regulates aggregation behavior. Dev. Biol. 298: 606-615 (2006).

Rhinn, M., & Dollé, P. Retinoic acid signalling during development. Development 139: 843-858 (2012).

Schilling, T. F., & Kinght, R. D. Origins of anteroposterior patterning and Hox gene regulation during chordate evolution. Phil. Trans. R. Soc. Lond. B 356 : 1599-1613 (2001).

Sugden, W. W., Leonardo-Mendonça, R. C., Acuña-Castroviejo, D., Siekmann, A. F. Genetic dissection of endothelial transcriptional activity of zebrafish aryl hydrocarbon receptors (AHRs). PLoS ONE 12(8): e0183433 (2017).

Yamamoto, T. Sex differentiation. In “Fish Physiology 3” Ed by W. S. Hoar, D. J. Randall, Academic Press, New York, pp 117-175. (1969).

Zerlin, M., Julius, M. A., & Kitajewski, J. Wnt/Frizzled signaling in angiogenesis. Angiogenesis 11: 63-69 (2008).

Figure 1. Development of CCV revealed by *vegfr1* expression

(A) Development of angioblasts expressing *vegfr1* was analyzed by *in situ* hybridization. Accumulation of angioblasts at PBA was marked by closed arrowheads. Primordial hindbrain channels (open arrowhead) and intersomite vessels (bracket) were also shown. **(B)** Percentage of embryos forming CCV.

Figure 2. RA controls CCV formation

(A) Embryos were treated with DEAB (10 μM) and RA (10 nM) at 10 hpf and examined at the indicated times for *vegfr1*+ angioblasts. The angioblasts accumulated at PBA (closed arrowhead) and primordial hindbrain channels (open arrowhead) were shown. Arrows indicate the position to which somites shift anteriorly. **(B)** Staged embryos were treated with DEAB (10 μM) and examined at 48 hpf for *vegfr1*+ angioblasts. Percentage of embryos showing no CCV was shown. * $p<0.005$, ** $p<0.00001$, n.s. not significant.

Figure 3. RA controls *ahr1* mRNA expression directly

(A) RNA was extracted from staged embryos from blastula to somite, and analyzed by RT-PCR for expression of the indicated genes. rRNA was used as a normalizing marker for the total RNA used. **(B)** The 22-hpf embryos were treated with cycloheximide (CHX) for 1 h, then with RA (10 nM) for 5 h before extraction of RNA. *ahr1* expression was analyzed by RT-PCR.

Figure 4. RA controls *ahr1* mRNA expression at PBA

(A) Staged embryos were analyzed for *ahr1* mRNA expression by *in situ* hybridization with sense and antisense probes. Expression at PBA was marked by bracket. **(B)** 10-hpf embryos were treated with the increasing concentrations of DEAB as indicated, and analyzed at 48 hpf. **(C, D)** Staged embryos were treated with DEAB (10μM) and analyzed at 48 hpf. *ahr1* expression (C). Percentage of embryos expressing no *ahr1* signal at PBA (D).

Figure 5. RA may control *ahr1* expression through RARα at PBA

In situ hybridization analysis of the indicated genes in 36-hpf embryos. **(A)** Specific expression of *krox20* at r3 and r5, *rarα* at r7 – r8 and its periphery in the hindbrain, and *raldh2* in the somite. **(B)** Effects of RA and DEAB on expression of *hoxa3a*. Anterior and posterior shifts of hindbrain are indicated by arrows. **(C)** Effects of DEAB and Ro41-5253 on expression of *raldh2*. Anterior shift of somite is indicated by arrow. **(D)** Effects of DEAB on expression of *rarα* and *rarγ1*. **(E)** Effects of DEAB on expression of *krox20* and *rarα*. Posterior shift of hindbrain is indicated by arrow. Addition of RA recovered *rarα* expression and hindbrain axis. **(F)** Effects of RA on expression of *krox20* and *rarα*. Anterior shift of hindbrain is indicated by arrow. **(G)** Staged embryos were treated with DEAB and analyzed for *rarα* expression.

Figure 6. *ahr1* is required for CCV formation

(A) Activation of *cyp1a* expression by treatment with β-NF at the indicated concentration during 10- to 36-hpf. **(B)** Activation of *cyp1a* expression by sense *ahr1* at 36 hpf. Transcript levels of *cyp1a* were normalized by β-actin controls. *, $p<0.01$. **(C)** Inhibition of *cyp1a* expression by antisense *ahr1* at 36 hpf. Normalized *cyp1a* transcript levels were also shown. *, $p<0.05$. **(D)** Percentage of embryos showing vascular damages at 3 dpf after the treatments indicated. **(E)** Percentage of embryos showing no *vegfr1*+ CCV at 48 hpf after the treatments indicated. **(F)** Inhibition of *vegfr1*+ CCV formation by cotreatment with 2 μM DEAB and antisense *ahr1*, which was rescued by sense *ahr1*. **(G)** Inhibition of CCV formation by treatment with 10 μM DEAB, which was not recovered by sense *ahr1*. Arrowhead, CCV.

Figure 7. A model for RA action in CCV formation

RA is required for *rarα* expression at posterior hindbrain (r7 - r8) and its periphery where *ahr1* expression is directly activated by RAR*α*. *ahr1*-expressing cells enhance the secretion of VEGF around them, which stimulates proliferation and migration of *vegfr1*-expressing angioblasts to accumulate angioblasts at PBA before the formation of CCV. *krox20* expression at r3 and r5, and *rarγ1* at the level of r5.

Figure S1. Introduction of DNA into embryos by electroporation

Schematic presentation of how to introduce DNA into medaka embryos by electroporation. The method consists of 4 steps as indicated. See text for detail.

Figure 1. Development of CCV revealed by *vegfr1* expression

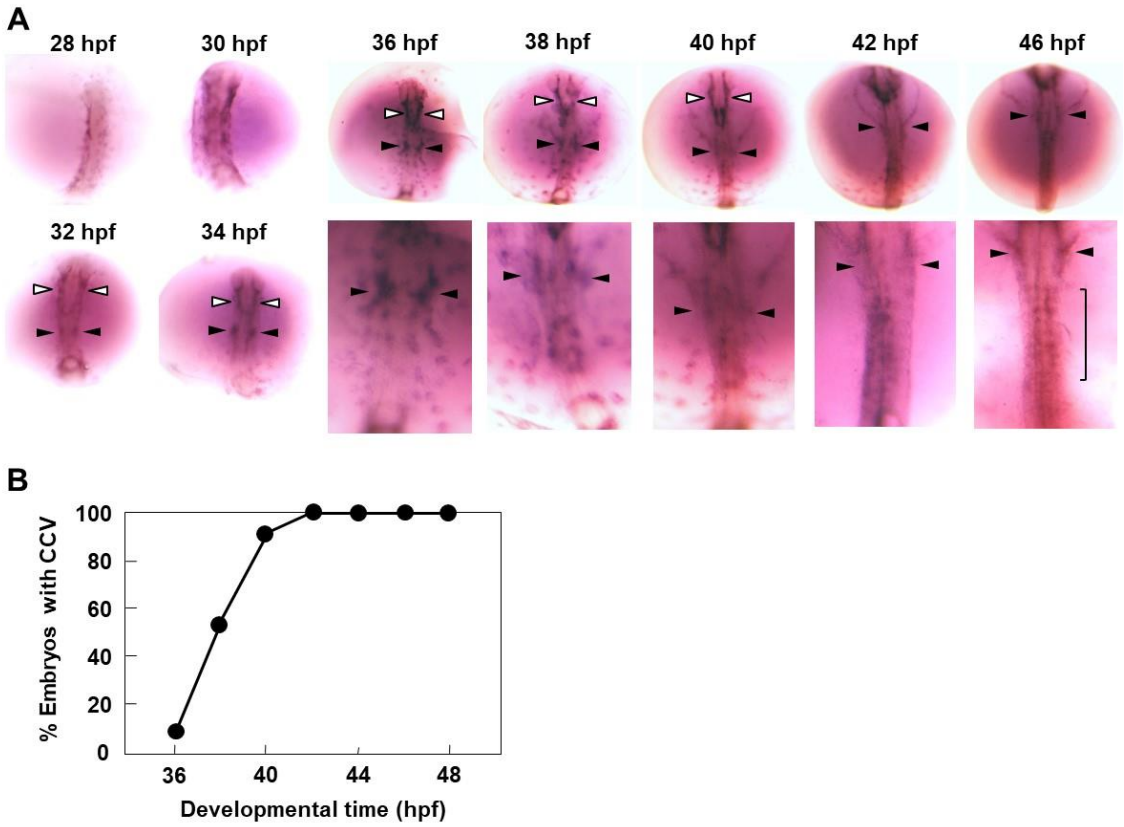

Figure 2. RA controls CCV formation

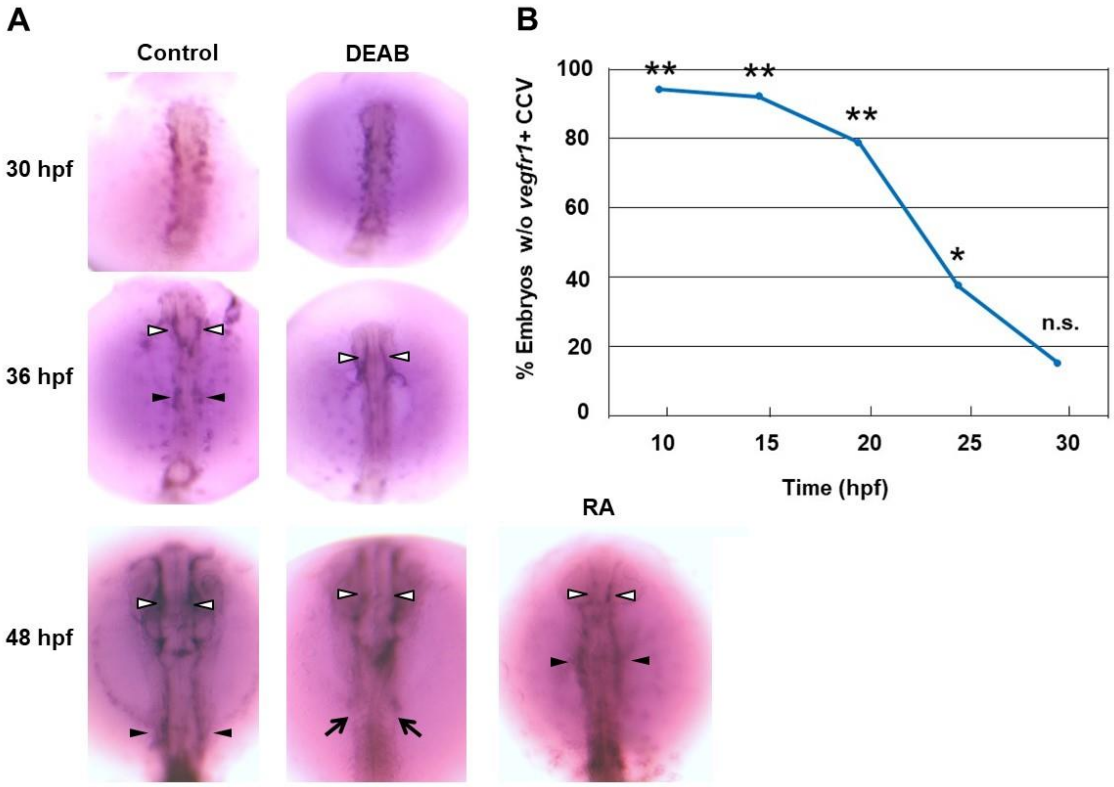

Figure 3. RA controls *ahr1* mRNA expression directly

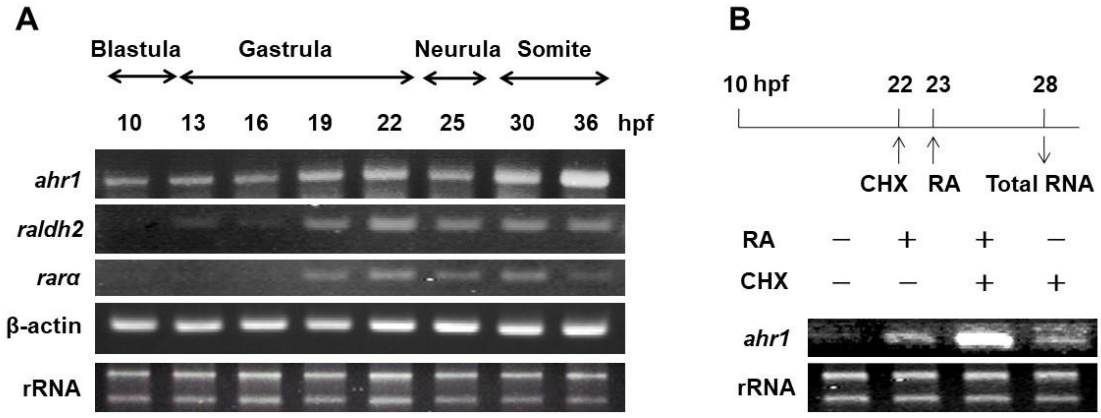

Figure 4. RA controls *ahr1* mRNA expression at PBA

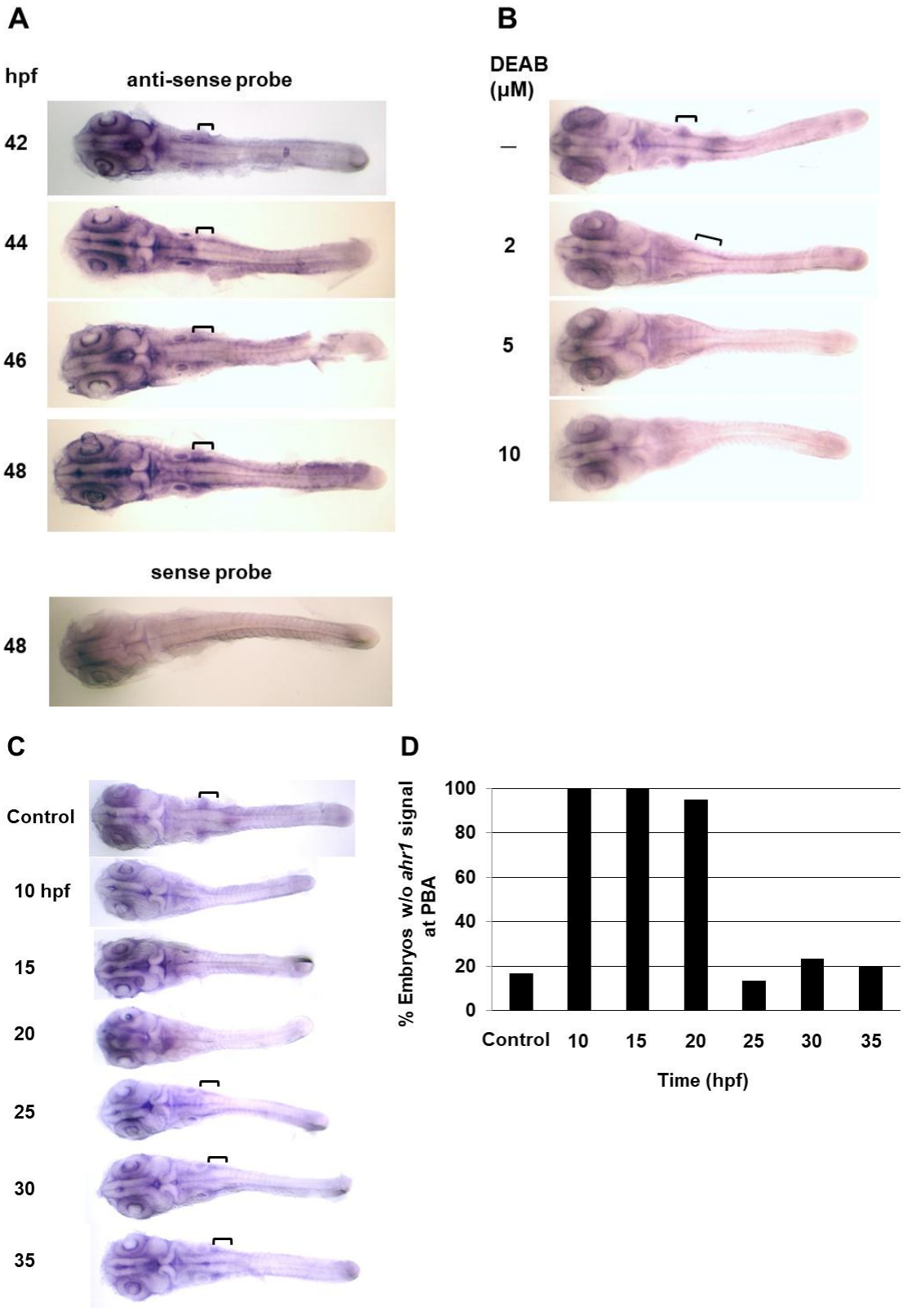

Figure 5. RA may control *ahr1* expression through RARα at PBA

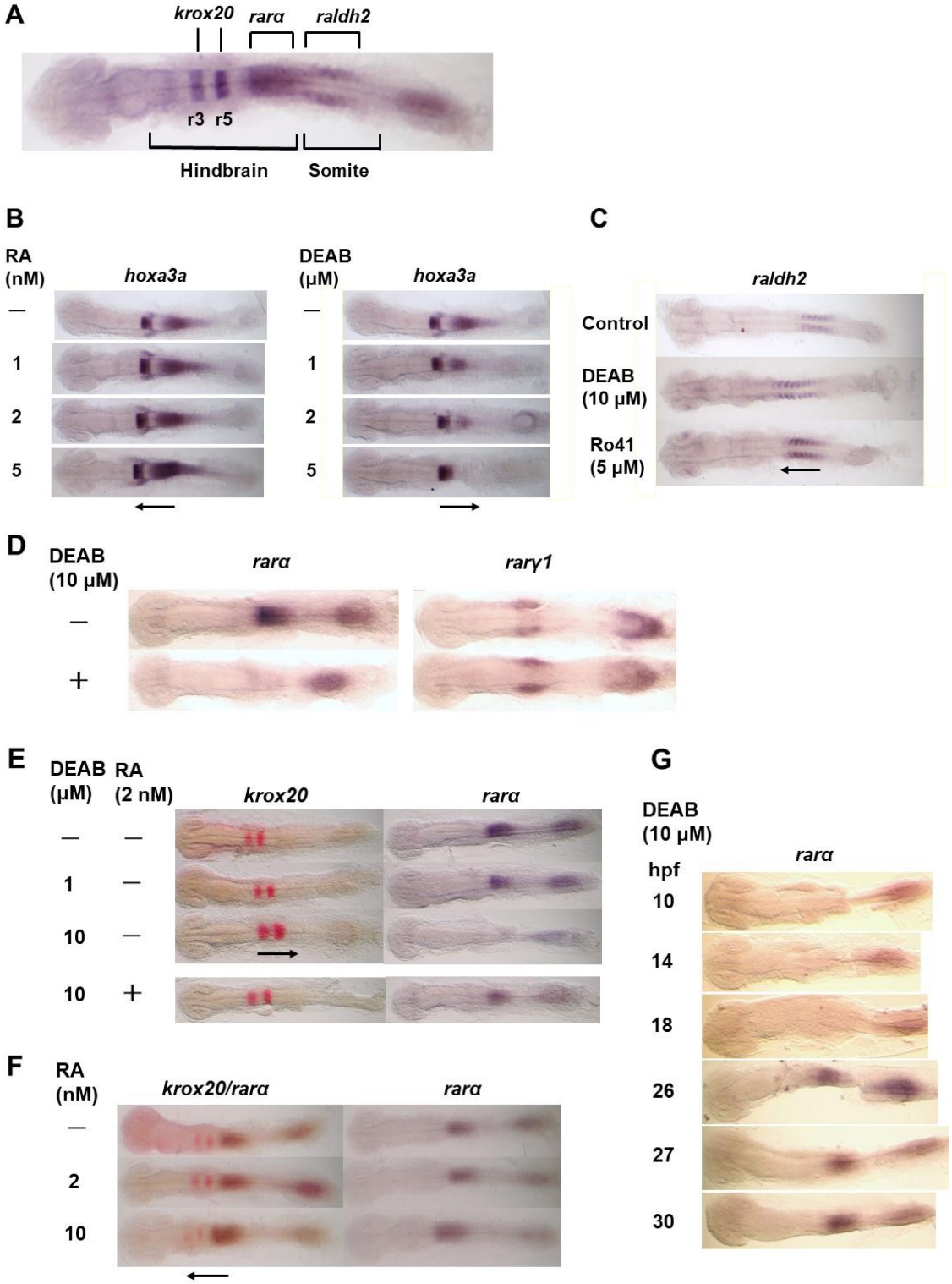

Figure 6. *ahr1* is required for CCV formation

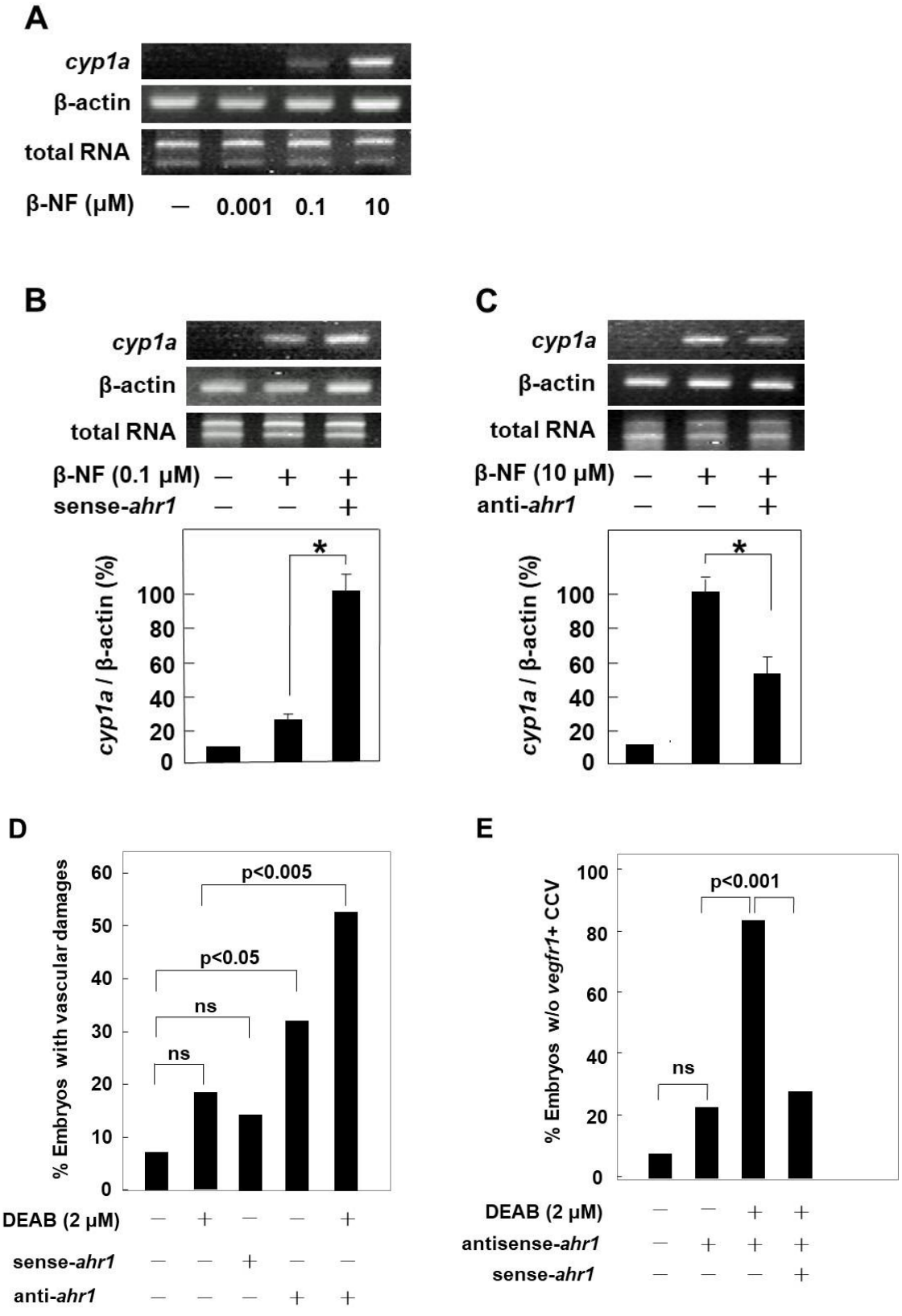

Figure 6. continued

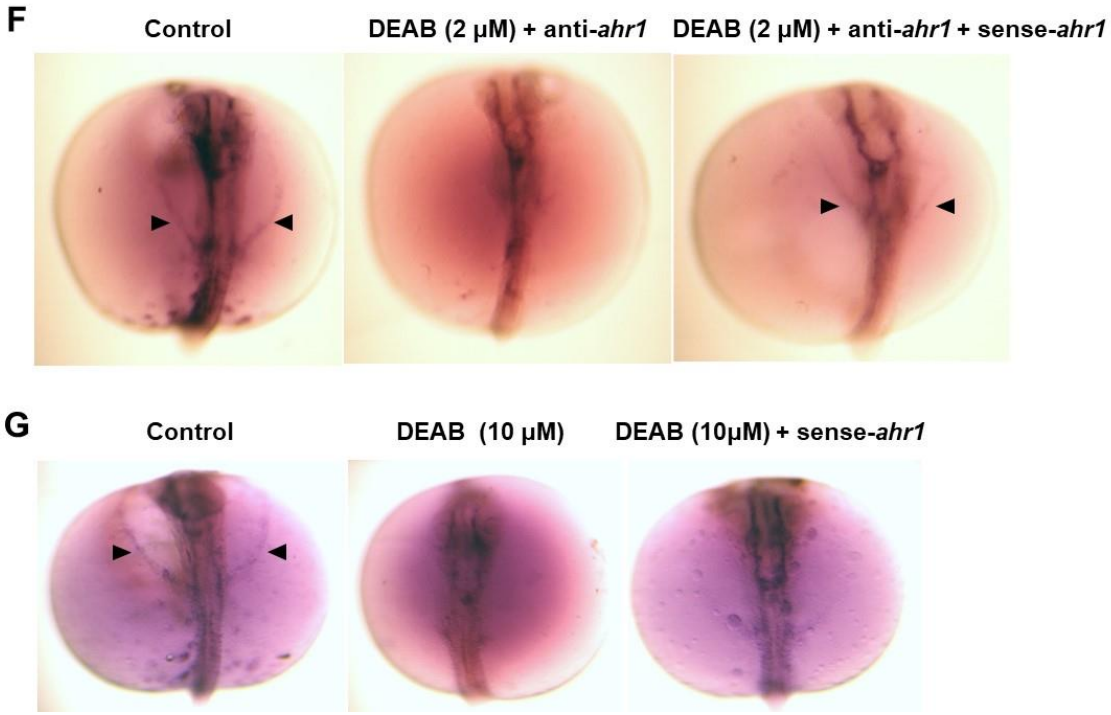

Figure 7. A model for RA action in CCV formation

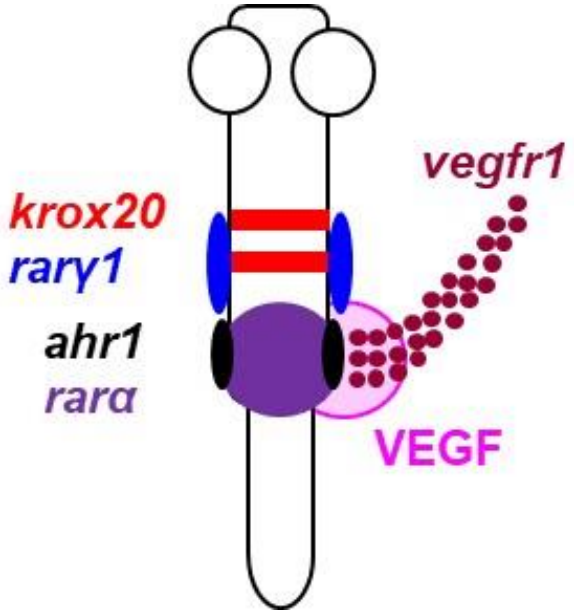

Figure S1. Introduction of DNA into embryos by electroporation